



## Letter

# Synthesis of yeast-assisted $\text{Co}_3\text{O}_4$ hollow microspheres—A novel biotemplating technique

Li Yang\*, Weisheng Guan, Bo Bai, Qing Xu, Yun Xiang

College of Environmental Sciences and Engineering, Chang'an University, Xi'an 710054, PR China

## ARTICLE INFO

## Article history:

Received 17 December 2009

Received in revised form 11 May 2010

Accepted 21 May 2010

Available online 27 May 2010

## Keywords:

Biotemplate

Yeast

$\text{Co}_3\text{O}_4$

Microsphere

## ABSTRACT

A novel technique for synthesis of biomorphic  $\text{Co}_3\text{O}_4$  hollow microspheres, using yeasts as bio-templates, has been successfully developed. Yeast cells were first coated with cobalt hydroxide chloride and then calcined to remove the templates for obtaining  $\text{Co}_3\text{O}_4$  hollow microspheres. The prepared products were examined by SEM, XRD and FT-IR for detailed structures. The SEM analysis showed that the products fully retained the morphology of the yeast cells and the size of the hollow microspheres was about  $3.7\ \mu\text{m}$  in length and  $2\ \mu\text{m}$  in width; XRD indicated that  $\text{Co}_3\text{O}_4$  hollow microspheres were of cubic phase; FT-IR revealed that some inherent functional groups on the surface of yeast cells, such as carbonyls, amines and hydroxyls etc., played major roles in the formation of  $\text{Co}_3\text{O}_4$  hollow microspheres. A possible formation mechanism of  $\text{Co}_3\text{O}_4$  hollow microspheres was proposed.

© 2010 Elsevier B.V. All rights reserved.

## 1. Introduction

Hollow micro-/nanostructures possess outstanding characteristics such as low density, high surface-to-volume ratio and low coefficients of thermal expansion that make them attractive for application in catalyst support, antireflection, surface coating, etc. [1]. In recent years, fabrication of hollow micro-/nanostructures using microbes as templates has become an active research area [2,3]. Microbes can easily be obtained in large amount in a short time without environmental pollution. Employing microbial cells as templates may significantly simplify the processing routes because both the synthesis of templates and modification of the template surface can be omitted [3,4]. These obvious advantages make microbes economical, environment-friendly, safe and time-saving candidates in directing the fabrication of various sophisticated architectures [5]. Till now, bio-templates including types of yeasts [3,4,6], bacteria [7–9], virus [10,11] and bacterial superstructures [12,13], have been successfully utilized to synthesize and pattern nanoparticles. Liu et al. [11] employed capsid shells derived from T7 bacteriophages to produce magnetic nanoparticles. And Mogul et al. [9] synthesized several microstructures with different morphology using several bacteria including *D. radiodurans*, *E. coli* and *R. rubrum* as biotemplates. Recently Cui et al. [4] reported the formation of hierarchical mesoporous  $\text{TiO}_2$  using yeasts via biomimetic mineralization. Our group has success-

fully prepared  $\text{Cr}_2\text{O}_3$  hollow microspheres by utilizing yeasts as biotemplates [3].

Tricobalt tetraoxide ( $\text{Co}_3\text{O}_4$ ), with its spinel structure, has been the target of chemists because of its promising application in gas-sensing, solar energy reflecting, catalysis and anode material in Li-ion rechargeable batteries [14–16]. Owing to the influence of particle size and morphology on the properties of materials, research has focused on synthesizing various  $\text{Co}_3\text{O}_4$  nanomaterials with special microstructures [17–19]. Up to now, a variety of synthetic pathways have been proposed for the formation of  $\text{Co}_3\text{O}_4$  hollow spheres [20–22]. The studies on the template-assisted formation of  $\text{Co}_3\text{O}_4$  hollow spheres mainly utilized conventional templates, such as SBA-15 silica [22], carbonaceous [21], PVP [23] and PS [24,25]. However, these approaches are usually multistep processes involving at least core formation and core surface modification. Hence, the development of simple preparation procedures of  $\text{Co}_3\text{O}_4$  hollow spheres should be of great significance.

In this paper, we describe a new template-directed method to fabricate  $\text{Co}_3\text{O}_4$  hollow microspheres using yeasts as templates. The objective of this study is to enlarge the variety of the biomorphic fabrication of metal oxide hollow structures.

## 2. Experimental

Yeast powder was purchased from Hebei Angel Company. Cobalt dichloride, ammonia and ethanol were provided by Shanghai Chemical Company. All the analytical chemicals were used as received without further purification. Double distilled water was used in all experiments.

In a typical procedure, 0.5 g of yeast powder (containing about  $1.4 \times 10^{10}$  yeasts), which was washed in physiological saline and ethanol each for three times, was dissolved in 30 ml of double distilled water. Then 1.2 g of  $\text{CoCl}_2 \cdot 6\text{H}_2\text{O}$  was added

\* Corresponding author. Tel.: +86 29 82339052; fax: +86 29 85585485.  
E-mail address: [yyangli@chd.edu.cn](mailto:yyangli@chd.edu.cn) (L. Yang).

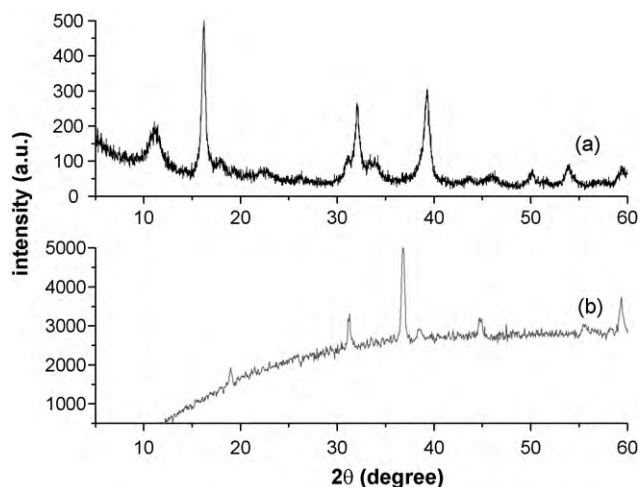


**Fig. 1.** XRD patterns of (a) hybrid precursors and (b) as-produced  $\text{Co}_3\text{O}_4$  particles.

into the solution. The system was then continuously magnetic stirred at  $60^\circ\text{C}$  for 3 h. Subsequently, the pH of the system was adjusted from 5.5 to 9 by ammonia. After aging, the mixture was centrifuged and washed with double distilled water and ethanol several times. After the products were dried at  $60^\circ\text{C}$ , they were calcined at  $400^\circ\text{C}$  for 3 h and allowed to cool at room temperature naturally in air.

The X-ray diffraction (XRD) patterns were recorded for phase identification on a Philips X'pert diffractometer with Cu-K $\alpha$  radiation ( $\lambda = 1.5418 \text{ \AA}$ ) which was operated at a voltage of 40 kV and a current of 40 mA. Scanning electron microscope (SEM) images were collected using scanning electron microscopy (VEGA II LMH, TESCAN). Fourier-transform infrared (FT-IR) spectroscopy measurements were recorded on a Nicolet NEXUS-670 instrument.

### 3. Results and discussion

#### 3.1. XRD

The XRD patterns of hybrid precursors and as-produced  $\text{Co}_3\text{O}_4$  hollow microspheres are shown in Fig. 1. The diffraction line of the hybrid precursors (Fig. 1a) can be assigned to the cobalt hydroxide chloride ( $\text{Co}_2(\text{OH})_3\text{Cl}$ ) phase (JCPD 73-2134). All the reflections in Fig. 1b can be readily indexed to a cubic phase of  $\text{Co}_3\text{O}_4$ , which are in agreement with the JCPDS No. 76-1802. No characteristic peaks of impurity phases are present, indicating the high purity of the

products. The crystallite size of the  $\text{Co}_3\text{O}_4$  particles can be estimated according to the line width analysis of the diffraction peaks based on the Scherrer equation:

$$D = \frac{k \cdot \lambda}{\beta \cdot \cos \theta} \quad (1)$$

where  $D$  is the crystallite size,  $\lambda$  is the wavelength of X-ray radiation (Cu K $\alpha$  radiation  $\lambda = 1.5418 \text{ \AA}$ ),  $k$  is a constant and usually taken as 0.89,  $\beta$  is the full width at half maximum (FWHM) after subtraction of equipment broadening, and  $\theta$  is the Bragg angle of peak. From the XRD results, the average size of the  $\text{Co}_3\text{O}_4$  building blocks is estimated to be around 24 nm.

#### 3.2. SEM

The SEM analysis was performed in order to have an insight into the morphology of the original yeasts, templates treated with cobalt ions, hybrid precursors and as-formed  $\text{Co}_3\text{O}_4$  particles, respectively. As shown in Fig. 2a, the original yeasts are oval and have smooth surfaces, and the length and width of the cells are about  $5 \mu\text{m}$  and  $4 \mu\text{m}$ , respectively. From Fig. 2b–d, we can see that the templates treated with cobalt ions, hybrid precursors and as-synthesized  $\text{Co}_3\text{O}_4$  particles retain the morphology of the yeast cells fairly well, but the dimension of particles and the roughness of the surface change considerably. Fig. 2b shows that the yeast templates treated with cobalt ions with relatively narrow size distribution are about  $3.3 \mu\text{m}$  in length and  $2.3 \mu\text{m}$  in width. And there are low ridges on the smooth surface of the particles. The reason for their reduction in dimension is that before being treated with cobalt ions, original yeasts were pretreated with ethanol to improve the biosorption of cobalt ions on cells. The pretreatment might result in the dehydration of cells and explain the decrease of particle size [26]. While the dimension of hybrid precursors after pH adjustment (Fig. 2c) increases to  $4.1 \mu\text{m}$  in length and  $2.8 \mu\text{m}$  in width. The slight increase in the size of hybrid precursors in comparison with yeast templates treated with cobalt ions provides assertive evidence that the cobalt hydroxide chloride nanoparticles have been attached to the surface of the yeast cores. These particles appear to have rough surface because they are core/shell structures and the biotemplates are covered with a rough  $\text{Co}_2(\text{OH})_3\text{Cl}$  shell. After calcinations the size of as-formed products (Fig. 2d) with good dispersion decreases to about  $3.7 \mu\text{m}$  in length and  $2 \mu\text{m}$  in width.

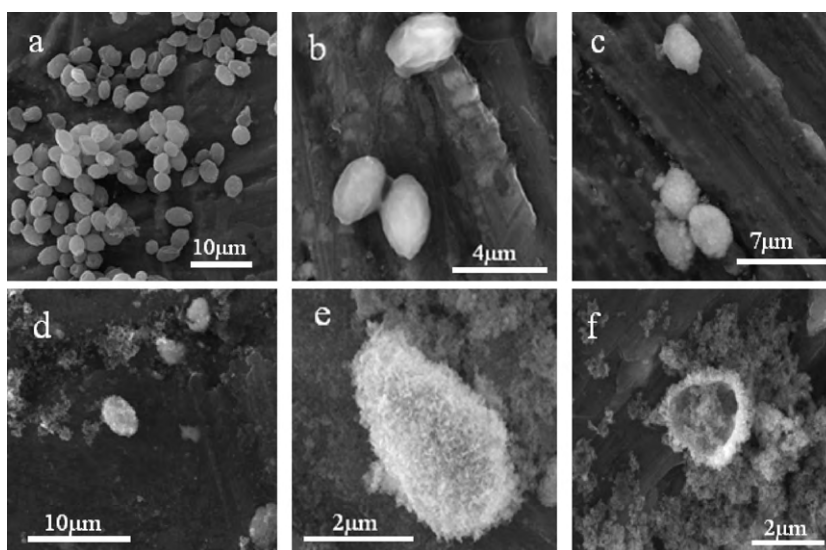


**Fig. 2.** SEM images of (a) original yeast templates, (b) yeast templates treated with cobalt ions, (c) hybrid precursors after pH adjustment, (d and e)  $\text{Co}_3\text{O}_4$  microspheres observed under different magnifications and (f) an individual broken  $\text{Co}_3\text{O}_4$  hollow microsphere.

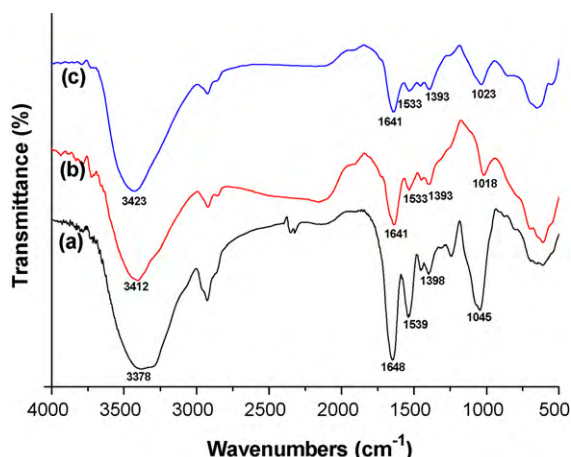


Fig. 3. Comparison of FT-IR spectra of (a) original yeasts, (b) yeasts treated with cobalt ions and (c) hybrid precursors.

Further enlargement of observation of the particle surface (Fig. 2e) reveals that the spheres have lamellar structures which are constructed by nanoparticles with diameter ranging from 20 nm to 30 nm. Fig. 2f shows an SEM image of a broken  $\text{Co}_3\text{O}_4$  microsphere, indicating that the as-prepared  $\text{Co}_3\text{O}_4$  particles are hollow and the wall thickness is about 0.32  $\mu\text{m}$ .

### 3.3. FT-IR

To understand the interactions between the cobalt ions and ingredients of yeast cell wall, FT-IR analysis was carried out on original yeasts, yeasts treated with cobalt ions and the hybrid precursors after pH adjustment, respectively.

The cell wall of yeasts is primarily made up of glucan, mannan, chitin and protein. And the reactive functional groups are essentially carbonyls, amines, hydroxyls and phosphoryl which are able to bind metal anions through coordination or electrostatic interactions [27–29]. Comparing Fig. 3a with Fig. 3b, we find several changes in the FT-IR spectrum of the yeast treated with cobalt ions. Firstly, the broad strong band at  $3378\text{ cm}^{-1}$  corresponding to the overlapping of  $-\text{NH}/-\text{OH}$  stretching of protein in yeast cells shifts to  $3412\text{ cm}^{-1}$  after cobalt uptake, which is due to the interaction of the cobalt ions with the  $-\text{NH}/-\text{OH}$  of protein on yeast cells [30]. Secondly, the dominating bends near  $1648\text{ cm}^{-1}$  and  $1539\text{ cm}^{-1}$  are assigned to the stretching band of  $\text{C}=\text{O}$ ,  $\text{C}-\text{N}$  from the amide I and amide II. These bends, the characteristic IR absorption of protein

in yeasts, shift from  $1648\text{ cm}^{-1}$  and  $1539\text{ cm}^{-1}$  to  $1641\text{ cm}^{-1}$  and  $1533\text{ cm}^{-1}$ . The red shifts indicate that the  $\text{C}=\text{O}$  and  $\text{C}-\text{N}$  bonds in peptides on yeast cell wall participate in the chelating bonds formation with the cobalt ions [31]. Additionally, the band at  $1398\text{ cm}^{-1}$  belonging to the symmetrical stretching bend of carboxyl shifts to  $1393\text{ cm}^{-1}$ , implying carboxyl as functional groups on yeast cells is also involved in the cobalt absorption [32]. Another shift from  $1045\text{ cm}^{-1}$  to  $1018\text{ cm}^{-1}$  corresponds to the interaction of cobalt ions with the oxygen of the hydroxyl group ( $\text{C}-\text{OH}$ ) from polysaccharides [33]. All of these changes show that at pH 5.5, cobalt ions would undergo surface preferred cooperation and interaction with some portion of the  $\text{CONH}/-\text{COO}^-$  groups of protein, polysaccharides, and other functional residues. The interaction between cobalt ions and bio-macromolecules could serve as the directors during the construction of biomorphic hierarchical nanomaterials.

By this method, after the system was adjusted to pH 9 by adding ammonia and aging, the hybrid precursors was synthesized. The FT-IR spectrum of as-formed hybrid precursors is showed in Fig. 3c. This spectral retains the tendency of the FT-IR spectrum of the yeast treated with cobalt ions at pH 5.5 (Fig. 3b). However, the intensity of characteristic bends at  $1641\text{ cm}^{-1}$ ,  $1533\text{ cm}^{-1}$  and  $1393\text{ cm}^{-1}$  increase to a certain extent. A possible explanation for this is that the hybrid precursors, after the pH adjustment, are structurally the yeasts coated with  $\text{Co}_2(\text{OH})_3\text{Cl}$  shell. Thus the absorbance of inherent functional groups on the yeast cells becomes weaker.

### 3.4. Mechanism

The formation mechanism of  $\text{Co}_3\text{O}_4$  hollow spheres via a three-step process is proposed and illustrated briefly in Fig. 4. In the first-step, cobalt ions existing in the form of  $[\text{Co}(\text{H}_2\text{O})_6]^{2+}$  combine with functional groups of carboxyl, amines and hydroxyls on the yeast cell walls which is explained in the FTIR analysis in details. This process produces the first hexaaquacobalt (II) ions encapsulation layer. In the second-step,  $\text{Co}_2(\text{OH})_3\text{Cl}$  forms both on the yeast cell walls and in the solution after adding ammonia, which is confirmed by the XRD results of hybrid precursors. In addition, this is supported by findings from experiments that the  $\text{Co}_2(\text{OH})_3\text{Cl}$  gives a deep blue coloration while the  $[\text{Co}(\text{H}_2\text{O})_6]^{2+}$  complex gives a light pink coloration [34]. In the process of aging,  $\text{Co}_2(\text{OH})_3\text{Cl}$  clusters formed on the cell walls are inclined to grow by colliding with other  $\text{Co}_2(\text{OH})_3\text{Cl}$  clusters according to the ripening and aggregation theory. Additionally, the original templates endow the hybrid precursor with a high surface-to-volume ratio which means that the  $\text{Co}_2(\text{OH})_3\text{Cl}$  cluster formed on the cell walls has a higher

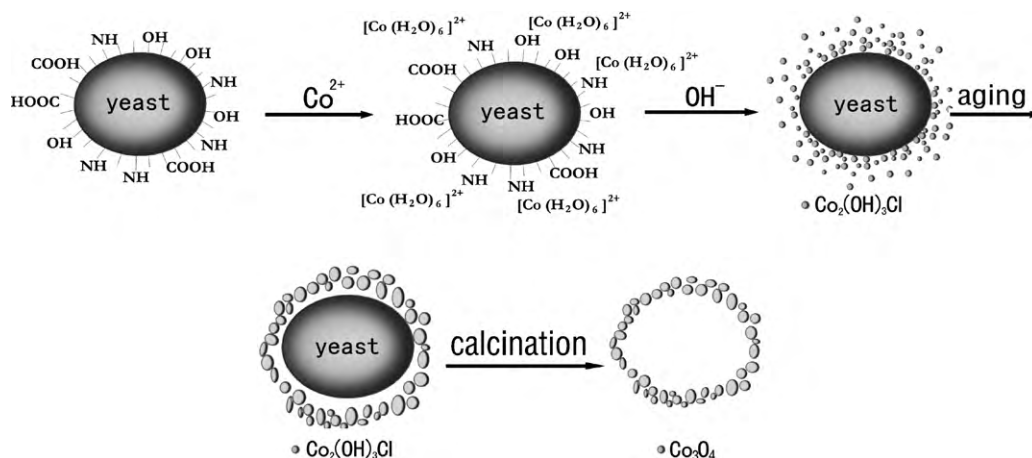
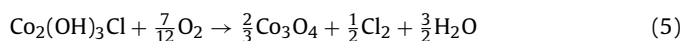
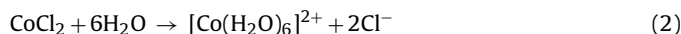


Fig. 4. Schematic illustration of  $\text{Co}_3\text{O}_4$  hollow microspheres formation.

efficiency and probability of colliding with other clusters in an appropriate concentration. As a result,  $\text{Co}_2(\text{OH})_3\text{Cl}$  covers the yeast cell walls and the hybrid precursors become bigger, which is confirmed by the results from XRD and SEM. Finally, the encapsulated microspheres were calcinated at  $400^\circ\text{C}$  to remove the yeast templates, and the subsequent dehydration and oxidization processes resulted in  $\text{Co}_3\text{O}_4$  hollow microspheres. The main reactions during the synthesis of  $\text{Co}_3\text{O}_4$  hollow microspheres were as follow:



Throughout the whole process, the yeasts not only served as support for the deposition of nanoparticles but also acted as hard templates to direct the morphology of the products.

#### 4. Conclusions

$\text{Co}_3\text{O}_4$  hollow spheres are first fabricated using yeasts as bio-templates based on the interaction between the inherent functional groups on the cell walls and the reactants. After calcinations at  $400^\circ\text{C}$  for 3 h, the templates are burned out leaving a central pore with a  $\text{Co}_3\text{O}_4$  shell remaining. The possible formation mechanism of  $\text{Co}_3\text{O}_4$  hollow spheres appears to be achieved through a three-step process. The result confirms a successful, simple and controllable method to fabricate  $\text{Co}_3\text{O}_4$  hollow spheres. This suggested route might open up an opportunity to fabricate other desired 3D structures using various microorganisms with different morphology as bio-templates.

#### Acknowledgements

The work is financially supported by the Program for Changjiang Scholars and Innovative Research Team in University of Ministry of Education of China (IRT0811) (PCSIRT) and Shaanxi Natural Science Foundation (No.2006Z06). The authors acknowledge professor Xun-Hong Chen in School of Natural Resources University of Nebraska-Lincoln for critical comments and suggestions on this paper.

#### References

- [1] X.W. Lou, L.A. Archer, Z. Yang, *Adv. Mater.* 20 (2008) 3987–4019.
- [2] T. Nomura, Y. Morimoto, H. Tokumoto, Y. Konishi, *Mater. Lett.* 62 (2008) 3727–3729.
- [3] B. Bai, P. Wang, L. Wu, L. Yang, Z. Chen, *Mater. Chem. Phys.* 114 (2009) 26–29.
- [4] J. Cui, W. He, H. Liu, S. Liao, Y. Yue, *Colloids Surf. B* 74 (2009) 274–278.
- [5] H. Zhou, T. Fan, D. Zhang, *Micropor. Mesopor. Mater.* 100 (2007) 322–327.
- [6] W. He, X. Tian, Y. Du, C. Sun, X. XudongZhang, S. Han, X. Han, X. Sun, Y. Du, Yue, *Mater. Sci. Eng. C* 30 (2010) 758–762.
- [7] H. Zhou, T. Fan, D. Zhang, Q. Guo, H. Ogawa, *Chem. Mater.* 19 (2007) 2144–2146.
- [8] Y. Zhang, E.-W. Shi, Z.-Z. Chen, B. Xiao, *Mater. Lett.* 62 (2008) 1435–1437.
- [9] R. Mogul, J.J. Getz Kelly, M.L. Cable, A.F. Hebard, *Mater. Lett.* 60 (2006) 19–22.
- [10] S.-Y. Lee, J.N. Culver, M.T. Harris, *J. Colloid Interface Sci.* 297 (2006) 554–560.
- [11] C. Liu, S.-H. Chung, Q. Jin, A. Sutton, F. Yan, A. Hoffmann, B.K. Kay, S.D. Bader, L. Makowski, L. Chen, *J. Magn. Magn. Mater.* 302 (2006) 47–51.
- [12] C. Fang, Y. Fan, J.M. Kong, G.J. Zhang, L. Linn, S. Rafeah, *Sens. Actuators B* 126 (2007) 684–690.
- [13] A. Rehman, Z.A. Raza, X. Saif-ur-Rehman, Z.M. Khalid, C. Subramani, V.M. Rotello, I. Hussain, *J. Colloid Interface Sci.* 347 (2010) 332–335.
- [14] J. Park, X. Shen, G. Wang, *Sens. Actuators B* 136 (2009) 494–498.
- [15] Z. Tian, N. Bahlawane, F. Qi, K. Kohse-Höinghaus, *Catal. Commun.* 11 (2009) 118–122.
- [16] J. Zheng, J. Liu, D. Lv, Q. Kuang, Z. Jiang, Z. Xie, R. Huang, L. Zheng, *J. Solid State Chem.* 183 (2010) 600–605.
- [17] G. Ji, Z. Gong, W. Zhu, M. Zheng, S. Liao, K. Shen, J. Liu, J. Cao, *J. Alloys Compd.* 476 (2009) 579–583.
- [18] J. Ma, S. Zhang, W. Liu, Y. Zhao, *J. Alloys Compd.* 490 (2010) 647–651.
- [19] A.A. Athawale, V. Singh, B.R. Mehta, K. Navinkiran, *J. Alloys Compd.* 492 (2010) 331–338.
- [20] F. Tao, C. Gao, Z. Wen, Q. Wang, J. Li, Z. Xu, *J. Solid State Chem.* 182 (2009) 1055–1060.
- [21] F. Teng, W. Yao, Y. Zheng, Y. Ma, T. Xu, G. Gao, S. Liang, Y. Teng, Y. Zhu, *Talanta* 76 (2008) 1058–1064.
- [22] G.J. Kim, X.-F. Guo, *J. Phys. Chem. Solids* 71 (2010) 612–615.
- [23] Y. Chen, Y. Zhang, S. Fu, *Mater. Lett.* 61 (2007) 701–705.
- [24] H. Yoshikawa, K. Hayashida, Y. Kozuka, A. Horiguchi, K. Awaga, S. Bandow, S. Iijima, *Appl. Phys. Lett.* 85 (2004) 5287–5289.
- [25] M. Ohnishi, Y. Kozuka, Q.-L. Ye, H. Yoshikawa, K. Awaga, R. Matsuno, M. Kobayashi, A. Takahara, T. Yokoyama, S. Bandow, S. Iijima, *J. Mater. Chem.* 16 (2006) 3215–3220.
- [26] Y. Zhang, W. Liu, M. Xu, F. Zheng, M. Zhao, *J. Hazard. Mater.* 178 (2010) 1085–1093.
- [27] Z. Lin, J. Wu, R. Xue, Y. Yang, *Spectrochim. Acta Part A* 61 (2005) 761–765.
- [28] J. Wang, C. Chen, *Biotechnol. Adv.* 24 (2006) 427–451.
- [29] M. Al-Saraj, M.S. Abdel-Latif, I. El-Nahal, R. Baraka, *J. Non-Cryst. Solids* 248 (1999) 137–140.
- [30] S. Tunali, T. Akar, A.S. Özcan, I. Kiran, A. Özcan, *Sep. Purif. Technol.* 47 (2006) 105–112.
- [31] V.K. Gupta, A. Rastogi, *J. Hazard. Mater.* 153 (2008) 759–766.
- [32] X. Han, Y.S. Wong, M.H. Wong, N.F.Y. Tam, *J. Hazard. Mater.* 146 (2007) 65–72.
- [33] Y.N. Mata, M.L. Blázquez, A. Ballester, F. González, J.A. Muñoz, *J. Hazard. Mater.* 158 (2008) 316–323.
- [34] Z. Zhao, F. Geng, J. Bai, H.-M. Cheng, *J. Phys. Chem. C* 111 (2007) 3848–3852.